Effects of Reaction Conditions on the Phenol Liquefaction of Peanut Shells

Shuguang Han,* Juqing Cui, Lu Gan, and Xiaoyan Zhou

Peanut shells were liquefied in phenol using sulfuric acid as the catalyst. The effects of the liquefaction conditions, such as the phenol/peanut shells ratio, catalyst loading, reaction temperature, and time, on the residue ratio, percent combined phenol, and formaldehyde reactivity of the liquefied products were investigated. The results showed that increasing the phenol/peanut shells ratio decreased the residue ratio and increased the combined phenol and formaldehyde reactivity. Increasing the catalyst loading decreased the residue ratio and increased the combined phenol, but a higher catalyst loading caused the formaldehyde reactivity to decrease. A higher reaction temperature and prolonged reaction time did not lead to a further decrease in the residue ratio and it further increased the combined phenol and formaldehyde reactivity. Fourier transform infrared spectroscopy and gas chromatography-mass spectroscopy showed that the liquefied products contained a large amount of polyphenol compounds and a small quantity of furan compounds and furfural. The SEM images showed small particles were the main portion of the liquefaction products and cellulose fibers could still be clearly seen.

INTRODUCTION

Phenolic resins, the first synthesized thermosetting resins, are still widely used in several applications, such as wood-based panel adhesives, coatings, and high-performance composite matrices. Phenolic resins are generally synthesized from phenol and formaldehyde. Phenol as a raw material for phenolic resins is produced from non-renewable fossil resources through the cumene method and crude phenol refining technology. The world reserves of economically exploitable fossil resources are finite, and the global expected consumption of fossil resources is gradually increasing. The phenol supply is challenged by the declining reserves of fossil resources. Under these circumstances, switching from fossil resources to renewable resources may provide an alternative way to deal with the sustainable growth requirements of organic raw materials (Karagöz *et al.* 2004; Ragauskas *et al.* 2006). Thus, the development of phenol alternatives from renewable resources has attracted great interest from both academic and industrial sectors.

Two approaches have been considered for obtaining renewable phenol alternatives. One approach is to extract chemical components, such as tannins, from wood, bark, or other plant resources that are rich in plant polyphenols (Pizzi 2006; Ping *et al.* 2011; Zhang *et al.* 2017a). The other method is to convert renewable biomass *via* various thermochemical processes (phenolysis, pyrolysis, *etc.*) into "bio-phenols" (Feng *et al.* 2015). Phenolysis is a liquefaction process conducted in phenol with an acidic catalyst at a

moderate temperature or without a catalyst at elevated temperatures to produce phenolic compounds (Feng *et al.* 2013). Acid-catalyzed phenol liquefaction of biomass is a well-known method with immense potential for substituting liquefied products for phenol to synthesize more environmentally-friendly phenolic resins (Alma *et al.* 1998; Alma and Basturk 2006; Ahmadzadeh *et al.* 2009; Pan *et al.* 2009; Lee *et al.* 2012; Li *et al.* 2012; Zhao *et al.* 2013; Yan *et al.* 2017). The products from white birch bark phenol liquefaction have been successfully applied in the synthesis of bark-based phenol formaldehyde resole, and the substitution rate of phenol was up to 50% (Feng *et al.* 2016). Phenol formaldehyde-type moldings, which are produced by liquefying wood into phenolic compounds with use of inorganic and organic acidic catalysts, have physical and mechanical properties that are comparable to those of commercial phenol-formaldehyde-type moldings (Alma *et al.* 1996a,b).

As the largest peanut producer in the world, China produces 5 million ton of peanut shells each year (Wu *et al.* 2015). Peanut shells are by-products of peanut production and are usually used as animal feed or fuel without any economic value-added applications (Xu *et al.* 2017). Furthermore, because the collection and disposal of this residue is generally becoming more difficult and expensive, large quantities of peanut shells are left without any treatment or simply burned in fields, which leads to various environmental problems (Biswas *et al.* 2017), such as air pollution and CO_2 emissions. The direct combustion of such residues in fields contributes 5% to 12% of the particulate matter concentration in the air, which has contributed to the recent severe hazy weather in China (Yao *et al.* 2010).

Peanut shells can be used as a precursor material to prepare biochar or activated carbon for the removal of heavy metals and some organic pollutants from contaminated water (Ahmad *et al.* 2012; Zhong *et al.* 2012; Zhang *et al.* 2014; Wu *et al.* 2015; Georgin *et al.* 2016; Chu *et al.* 2017; Xu *et al.* 2017), for generating high energy density liquid fuel by pyrolysis as a substitute for fossil fuels (Zhang *et al.* 2011; Gurevich Messina *et al.* 2015; Gurevich Messina *et al.* 2017), and they can be liquefied to polyol by polyethylene glycol 400 and glycerol for use in preparing rigid polyurethane foams (Zhang *et al.* 2016; Zhang *et al.* 2017b). Additionally, peanut shells can be converted into a phenol alternative *via* various thermochemical conversions, such as pyrolysis (Alma and Kelley 2002; Mamaeva *et al.* 2017). However, all of these methods still cannot consume all of the excess peanut shells. Many attempts at phenolysis have established that almost all lignocellulosic biomass can be successfully liquefied in phenols (Alma and Acemioglu 2004). Compared with wood and bark, peanut shells are more abundant in lignin and polyphenols (Gao *et al.* 2011; Zhang *et al.* 2013), which makes them suitable for phenolysis (Effendi *et al.* 2008; Feng *et al.* 2013). However, there have only been a few studies that focused on the liquefaction of peanut shells in phenol. Considering the large annual output of peanut shells worldwide, it would be highly beneficial to explore phenol liquefaction as a method to convert this waste to a useful feedstock for large-scale industrial applications, such as making wood adhesives. Yet, it is still unclear how the reaction conditions affect the liquefaction yield and liquefied products when peanut shells are used.

Therefore, in this study, peanut shells were liquefied in phenol with an acid catalyst. The effects of different liquefaction reaction conditions on the residue ratio, percent combined phenol, and formaldehyde reactivity of the liquefied peanut shell fraction were investigated to better understand the efficacy of phenol liquefaction as a conversion technique for peanut shells.

EXPERIMENTAL

Materials

Peanut shells were purchased from a farmer's market in Nanjing, China. They were washed with deionized water to remove impurities from the surface, dried in an oven at 105 °C for 12 h, then crushed and sieved through a 100-mesh sieve. The portion with particle size greater than 100-mesh was used for liquefaction. The peanut shells were found to contain 61.8 wt.% holocellulose measured according to the Chinese national standard GB/T 2677.10 (1995), 34.4 wt.% acid insoluble lignin measured according to the Chinese national standard GB/T 2677.8 (1994), 4.46 wt.% ethanol-toluene extractives measured according to the Chinese national standard GB/T 2677.6 (1994), and 3.45 wt.% ash measured according to the Chinese national standard GB/T 2677.3 (1993). Phenol, concentrated sulfuric acid (96%), formaldehyde solution (37%), methanol, and other chemicals were used as analytical reagents without further purification (Aladdin Company, Shanghai, China).

Methods

Preparation of the phenol liquefied peanut shells

The phenol and peanut shells were added to a three-necked flask equipped with a reflux condenser and stirrer. The reaction was performed in a heating oil bath at the settled temperature (140, 160, 180 °C) under atmospheric pressure. After the liquefaction reaction, the system was cooled down to room temperature using cold water.

To investigate the effect of different liquefaction reaction conditions on the residue ratio, percent combined phenol, and formaldehyde reactivity of the liquefied peanut shells, 100 g of peanut shells were used for each experiment and the experiments were conducted following an L_9 (3^4) orthogonal design. The liquid to solid ratio (phenol/peanut shells, w/w) (A), catalyst loading (loading rate of sulfuric acid as a catalyst, based on the weight of the peanut shells, %) (B), liquefaction reaction temperature (°C) (C), and liquefaction reaction time (min) (D) were selected as the four factors with three levels for the orthogonal experiment. The orthogonal experiment factors and levels are shown in Table 1. The experiment scheme is shown in Table 2, and to assure the accuracy of the experimental data, each experimental group had three replicates.

Table 1. Factors and Levels for the Orthogonal Experiment of Phenol Liquefaction of Peanut Shells

| Level | Factor | | | |
| | A | B | C | D |
	Liquid to Solid Ratio (w/w)	Catalyst Loading (%)	Liquefaction Reaction Temperature (°C)	Liquefaction Reaction Time (min)
1	2	6	140	60
2	3	8	160	80
3	4	10	180	100

Measurement of the residue ratio

The liquefied products were diluted using excessive methanol, and then they were vacuum filtered using a vacuum pump and millipore filter paper to separate the solid residue (methanol-insoluble part) from the methanol-soluble part. Simultaneously, the

filter residue was washed in methanol until the filtrate ran clear. The methanol-insoluble residue was dried in an oven at 105 °C to a constant weight. The residue ratio was calculated using Eq. 1,

$$R = W_r / W_o \times 100\% \tag{1}$$

where R is the residue ratio of the peanut shells in the liquefaction reaction (%), W_r is the oven-dried weight of the methanol-insoluble residue after liquefaction (g), and W_o is the original oven-dried weight of the peanut shells before liquefaction (g).

After the methanol was removed from the filtrate by distillation under vacuum, the remaining liquefied peanut shells were used for further analysis.

Measurement of the percent combined phenol of the liquefied peanut shells

The amount of free phenol remaining in the methanol-soluble shells was first measured by using high performance liquid chromatography (HPLC) (1260 Infinity, Agilent, Santa Clara, USA) with a DAD ultraviolet-visible detector (254 nm) and ZORBAX Eclipse plus C18 column (4.6 mm × 100 mm, 5 µm) (Agilent, Santa Clara, USA). Measurements were done at 40 °C and a flow rate of 1.0 mL/min using a methanol/water solution (1/2, v/v) as the mobile phase. The methanol-soluble liquefied products were dissolved in methanol at a concentration of 0.1% and 10 mL were injected into the HPLC apparatus. Meanwhile, solutions of pure phenol at different methanol concentrations (0.1%, 0.2%, 0.3%, 0.4%, 0.5%, and 0.6%) were used as standard solutions for calibration purposes. The percent combined phenol was calculated using Eq. 2,

$$C_p = (P_o - P_f) / (P_o + W_o - W_r) \times 100\% \tag{2}$$

where C_p is the percent combined phenol (%), P_o is the initial amount of phenol (g), and P_f is the amount of phenol remaining after liquefaction (g).

Measurement of the formaldehyde reactivity of the liquefied peanut shells

The formaldehyde reactivity of the liquefied peanut shells was determined using the hydroxymethylation reaction method. The liquefied peanut shells were hydroxymethylated by the reaction for 5 h at 60 °C with excessive formaldehyde in the presence of sodium hydroxide solution (50%, w/w) and a ratio of liquefied peanut shells to excessive formaldehyde to sodium hydroxide solution of 10:30:10 (g, w/w). Briefly, 10 g of the liquefied peanut shells was added to a 500 mL conical flask. 30 g of formaldehyde solution (37%, w/w) and 10 g of sodium hydroxide solution (50%, w/w) were added to the conical flask. The mixture was reacted in a thermostatic water bath through condensate reflux device at 60 °C for 5 h. After reaction finished, cooling the entire reaction system for 30 min, then using 150 mL of distilled water to swash glass wall and dilute the reaction system. The filtrate was collected through a funnel. The free formaldehyde content in the filtrate was determined by the sodium sulfite method, according to the Chinese national standard GB/T 14074 (2006). The formaldehyde reactivity was calculated using Eq. 3,

$$F_r = (F_e - F_f) / (P_o + W_o - W_r) \times 100\% \tag{3}$$

where F_r is the formaldehyde reactivity of the liquefied peanut shells (%), F_e is the weight of the excessive formaldehyde (g), and F_f is the weight of the free formaldehyde (g).

FTIR measurements

The FTIR measurements of the peanut shell powder, liquefied peanut shells, and residue were done using an FTIR TENSOR 27 spectrometer (Bruker, Karlsruhe, Germany) over a frequency range of 4000 cm^{-1} to 400 cm^{-1}. The samples were dried under vacuum freezing and the KBr pellet method was used for sample preparation.

GC-MS analysis of the liquefied peanut shells

The chemical composition of the liquefied peanut shells was analyzed using GC-MS (Agilent 7890A/5975C, Santa Clara, USA) with a 30-m × 0.25-mm × 0.25-μm capillary column (DB-5ms, Agilent, Santa Clara, USA). Helium (99.999 %) was used as the carrier gas with a constant flow of 1.0 mL/min. For all analysis, the samples were dissolved in a mixture of dichloromethane and methanol (1:1 v/v, p.a. grade) to a concentration of approximately 0.1 mg/mL from where 1.0 μL of this solution was introduced to the GC-MS. The oven was programmed to increase at a rate of 5 °C/min until it reached a final temperature of 250 °C, which was held for 20 min. The compounds were identified by comparison with the NIST17 library (reference).

SEM observation of the liquefaction products

Scanning electronic microscopy (SEM) (JSM-7600F, Hitachi, Tokyo, Japan) was used to examine the morphology of the liquefaction products. The samples were dried under vacuum freezing, and sputter coated with gold prior to scanning.

RESULTS AND DISCUSSION

Analysis of the Orthogonal Experiment

From Table 2, it was suggested that the liquid to solid ratio had the most impact on the residue ratio and formaldehyde reactivity. The catalyst loading was found to markedly affect the percent combined phenol. Furthermore, it was concluded from the range analysis that the liquefaction conditions for the minimum residue ratio, maximum percent combined phenol, and maximum formaldehyde reactivity were $A_3B_3C_2D_3$, $A_3B_3C_3D_3$, and $A_3B_2C_2D_2$, respectively. From the point of view of substituting phenol for phenolic resin synthesis, $A_3B_2C_2D_2$ seemed to be the most reasonable liquefaction conditions, whose levels were a liquid to solid ratio of 4, catalyst loading of 8%, liquefaction reaction temperature of 160 °C, and liquefaction reaction time of 80 min.

Effect of the Reaction Conditions on the Residue Ratio, Percent Combined Phenol, and Formaldehyde Reactivity

Residue ratio

The effect of the phenol to peanut shells ratio on the residue ratio from liquefaction is shown in Fig. 1 (line A). The residue ratio consistently decreased as the phenol to peanut shells ratio increased from 2 to 4, and a remarkable reduction in the residue ratio was observed when the phenol to peanut shells ratio increased from 2 to 3. When the phenol to peanut shells ratio exceeded 3, the level of reduction was not notable, even though the residue ratio decreased further. The same trend also appeared during wood liquefaction in phenol (Lin *et al.* 1994; Pan *et al.* 2007; Zhao *et al.* 2013). The peanut shell components underwent decomposition, phenolation, and recondensation during liquefaction. When the liquid ratio was lower than a certain value and as the liquefaction reaction time increased,

recondensation of the liquefied peanut shell components became the preferable reaction, rather than phenolysis. Meanwhile, decomposition and recondensation are competing reactions, and a higher amount of phenol used in the liquefaction retarded the recondensation reactions among the degraded components and prevented the formation of new larger molecular weight insoluble residues (Lin *et al.* 1997).

Table 2. L_9 (3^4) Orthogonal Experiment Scheme and Results

Experiment No.	A	B	C	D	R (%)	C_p (%)	F_r (%)
1	2	6	140	60	30.7 ± 0.2	43.6 ± 0.3	47.1 ± 0.1
2	2	8	160	80	21.4 ± 0.1	60.1 ± 0.1	59.5 ± 0.1
3	2	10	180	100	20.3 ± 0.2	67.4 ± 0.2	55.2 ± 0.3
4	3	6	160	100	11.8 ± 0.3	61.9 ± 0.4	55.5 ± 0.2
5	3	8	180	60	13.3 ± 0.3	65.7 ± 0.1	63.1 ± 0.3
6	3	10	140	80	12.8 ± 0.2	63.4 ± 0.1	59.8 ± 0.2
7	4	6	180	80	12.4 ± 0.1	62.1 ± 0.2	60.4 ± 0.5
8	4	8	140	100	12.6 ± 0.1	63.8 ± 0.1	67.7 ± 0.2
9	4	10	160	60	11.6 ± 0.4	68.5 ± 0.1	64.6 ± 0.2
[a]K1^R	24.133	18.3	18.7	18.533			
K2^R	12.633	15.767	14.933	15.533			
K3^R	12.2	14.9	15.333	14.9			
R^R	11.933	3.4	3.767	3.633			
[b]K1^P	57.04	55.88	56.93	59.293			
K2^P	63.677	63.22	63.52	61.883			
K3^P	64.827	66.443	65.093	64.367			
R^P	7.787	10.563	8.163	5.074			
[c]K1^F	53.933	54.333	58.2	58.267			
K2^F	59.467	63.433	59.867	59.9			
K3^F	64.233	59.867	59.567	59.467			
R^F	10.3	9.1	1.667	1.633			

A, B, C, and D denote liquid to the solid ratio, the catalyst loading, the liquefaction reaction temperature and the liquefaction reaction time, respectively; R, C_p, and F_r denote the residue ratio, the percent combined phenol and the formaldehyde reactivity, respectively; Values are the mean ± standard deviation of three replicates; [a] K1^R, K2^R, and K3^R denote the average residue ratio for levels 1, 2, and 3, respectively; R^R denotes the residue ratio range; [b] K1^P, K2^P, and K3^P denote the average percent combined phenol of levels 1, 2, and 3, respectively; R^P denotes the range of percent combined phenol; [c] K1^F, K2^F, and K3^F denote the average formaldehyde reactivity of levels 1, 2, and 3, respectively; R^F denotes the range of formaldehyde reactivity.

The effect of the catalyst loading on the residue ratio from liquefaction is shown in Fig. 1 (line B). When the catalyst loading increased, the residue ratio decreased gradually. A higher catalyst loading promoted the extent of liquefaction through hydrolysis and degradation of the cellulose and hemicellulose, but recondensation between the phenol and

decomposed products occurred at a rather high catalyst dosage, which led to the residue ratio decreasing slowly.
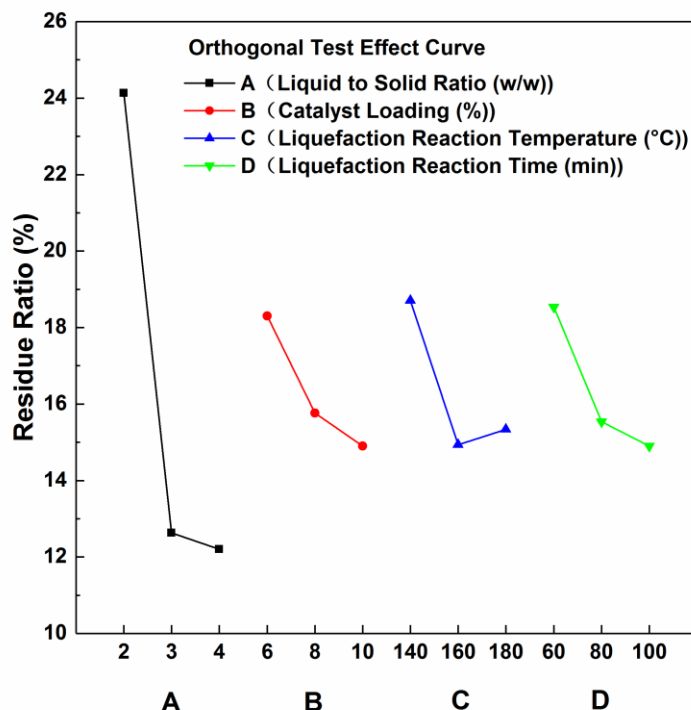

Fig. 1. Effects of the reaction conditions on the residue ratio of the peanut shell liquefaction

Figure 1 (line C) shows the relationship between the residue ratio and liquefaction temperature. When the liquefaction temperature was increased from 140 °C to 160 °C, the residue ratio decreased noticeably and reached a minimum value. When the liquefaction temperature was increased from 160 °C to 180 °C, the residue ratio increased slightly. It was reported that the recondensation reaction among the decomposed components might have occurred at 180 °C, which could have affected the residue ratio (Pan *et al.* 2007).

Figure 1 (line D) shows that with an increasing liquefaction reaction time, the residue ratio decreased, especially from 60 min to 80 min. When the reaction time was increased from 80 min to 100 min, there was only a minor change in the residue ratio. The liquefaction efficiencies were not remarkably improved by increasing the liquefaction time when the liquefaction reaction time reached a reasonable value.

Percent combined phenol

Figure 2 (line A) shows that the percent combined phenol increased as the phenol to peanut shells ratio increased. Higher phenol/peanut shells ratios promoted liquefaction and retarded the secondary condensation reaction of the decomposed components, which resulted in more percent combined phenol after liquefaction. For the acid-catalyzed phenol liquefaction, the phenol acted not only as a liquefaction solvent, but also as a cross-linker for the degraded components (Zhang *et al.* 2006). Figure 2 (line B) shows that the catalyst loading was the most effective factor that affected the percent combined phenol, as it increased remarkably when the catalyst loading increased.

A higher catalyst loading promoted liquefaction of the lignin and hydrolysis of the hemicellulose and cellulose. The acid catalyst not only catalyzed the liquefaction reaction, but it also played a major role in accelerating recondensation reactions among the degraded components and phenol. Figure 2 (lines C and D) shows that the reaction temperature and reaction time had a similar trend effect on the percent combined phenol. With higher reaction temperatures and longer reaction times, the phenol reacted more with the peanut shell components during liquefaction. The percent combined phenol increased gradually with an increasing reaction temperature and time.
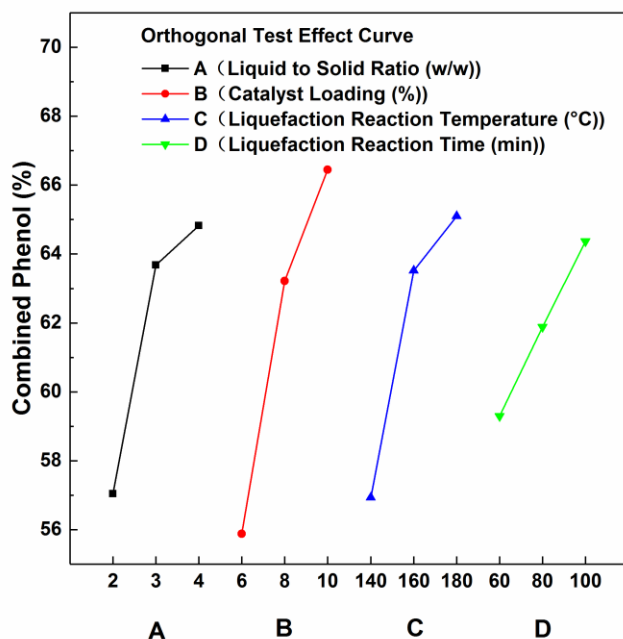

Fig. 2. Effects of the reaction conditions on the percent combined phenol from peanut shell liquefaction

Formaldehyde reactivity

The formaldehyde reactivity of the liquefied products was determined to formulate resins that can assist in the preparation of bio-based phenolic resins. Figure 3 (line A) shows that the formaldehyde reactivity of the liquefied peanut shells linearly increased as the phenol to peanut shells ratio increased. Because phenol was added as the liquefaction solvent, the amount of formaldehyde consumed by the reaction accounted for the phenol content, which had three reactive sites. The formaldehyde consumption levels generally agreed with the amount of phenol used during liquefaction (Hassan *et al.* 2009).

Figure 3 (line B) shows the relationship between the formaldehyde reactivity and catalyst loading. When the catalyst loading increased from 6% to 8%, the formaldehyde reactivity increased remarkably and reached a maximum value. When the catalyst loading increased from 8% to 10%, the formaldehyde reactivity decreased. Liquefaction broke down the lignin and carbohydrates, and the acid catalyst played a major role in accelerating recondensation reactions among the degraded components and phenol. There was the possibility of some phenol reacting with the liquefaction products and deriving a high molecular weight polymer that was not be an active site for formaldehyde reaction. For that reason, higher reaction temperatures and prolonged reaction times had similar trend effects on the formaldehyde reactivity.
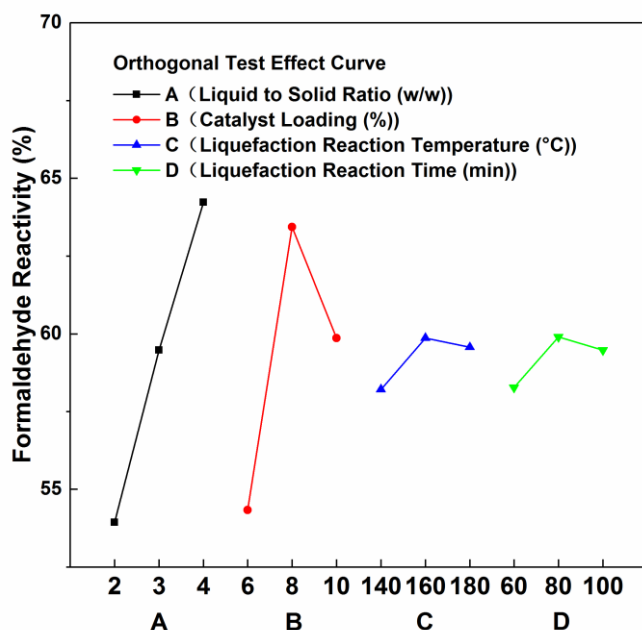
Fig. 3. Effects of the reaction conditions on the formaldehyde reactivity of peanut shell liquefaction

FTIR analysis

Figure 4 shows three FTIR spectra of the raw peanut shells, liquefied peanut shells, and residue. The OH and CH_2 group stretching vibrations had peaks at 3442 cm^{-1} and 2925 cm^{-1}, respectively. Stretching vibration peaks at 1635 cm^{-1} and 1124 cm^{-1} were attributed to C=O and C-O bonds present in the celluloses, respectively, and the sharp peak indicated some residual celluloses that were un-liquefied in the phenol might have been present in the liquefaction products and residue.

The absorption bands at 1511 cm^{-1}, 1452 cm^{-1}, and 831 cm^{-1} representing benzene rings were seen in spectra a and b, but completely disappeared in spectrum c, which indicated that all of the lignin was sufficiently liquefied (Long *et al.* 2015). The band at 1382 cm^{-1} was associated with crystalline cellulose, and the intensity of this band was more pronounced in spectra a and c compared with in spectrum b, which may have been because of the high cellulose content.

The absorbance peaks at 1228 cm^{-1} and 1035 cm^{-1} represented the C-O-C unit attributed to aryl-alkyl ether linkages in the lignin. The absorbance peak at 1170 cm^{-1} was attributed to the skeletal pyranose ring with C–O–C stretching vibration (Yang *et al.* 2007). The peaks at 752 cm^{-1} and 693 cm^{-1} represented C-H in the benzene rings and were seen in spectrum b, which when combined with the absorption peak at 3442 cm^{-1}, indicated that the liquefaction reaction led to the degradation of lignin and that the liquefaction products consist of polyphenols.
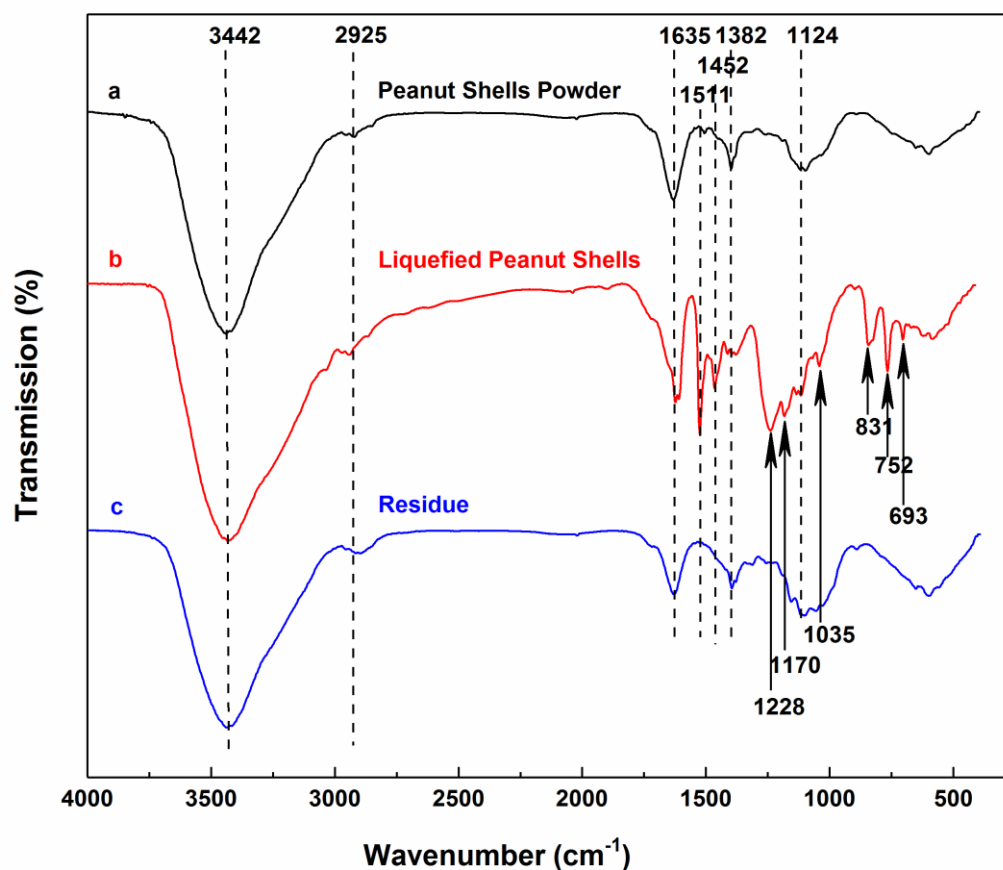
Fig. 4. FTIR spectra of the raw peanut shells, liquefied peanut shells, and residue; liquefaction conditions: phenol/peanut shells ratio = 4, catalyst loading = 8%, reaction temperature = 160 °C, and reaction time = 80 min

GC-MS analysis of the liquefied peanut shells

The products from liquefaction of the peanut shells were determined using GC-MS. The results are presented in Table 3 and show that more than 20 kinds of aromatic products were detected, among which the phenolic monomer was dominant. Aromatic acid ethylester, ketone, furan compounds, furfural, and ester were also detected. The results listed in Table 3 indicated that all of these aromatic structural units originated from liquefaction of the lignin, the furan compounds came from liquefaction of the celluloses, and the presence of furfural was attributed to liquefaction of the hemicelluloses.

SEM observation of the liquefaction products

Figure 5 shows SEM images of the liquefaction products generated with a phenol/peanut shells ratio of 4, catalyst loading of 8%, reaction temperature of 160 °C, and reaction time of 80 min. Small particles were the main portion of the liquefaction products and the cellulose fibers could still be clearly seen. It was interpreted that the liquefaction conditions dissolved lignin preferentially, which was the most sensitive part of phenol liquefaction. Meanwhile, the cellulose, considered to be the hardest part of phenol liquefaction, became part of the residues.

Table 3. GC-MS Spectrum Analysis of the Liquefied Peanut Shells

Reaction Time (s)	Compound	Structure	Area (%)
3.65	1,3-Diethoxy-1,1,3,3-tetramethyldisiloxane		0.09
4.48	Phenol		76.72
5.90	Guaiacol		0.74
10.24	2-Acetylbenzofuran		0.13
10.91	Dimethyl phthalate		0.71
15.64	1,3-Naphthalenediol;		0.11
16.54	Benzenemethanol,2,2'-oxybis-		0.28
16.76	Ethyl palmitate		0.19
16.96	2,2'-methylenebis-Phenol		1.39
17.26	Phenol,2-[(4-hydroxyphenyl)methyl]-		6.92
17.28	Furfural		1.2
17.91	4,4'-methylene diphenol		0.44
18.37	4,4'-ethylidenebis-Phenol		0.45
18.58	2-Propen-1-one,1-(4-hydroxyphenyl)-3-phenyl-		0.57
18.75	Dibenz[b,e]oxepin-11(6H)-one		0.16
19.73	Diphenic acid		0.18
26.26	1,1,2,2-Tetrakis(4-hydroxyphenyl)ethane		0.51

Liquefaction conditions: phenol/peanut shells ratio = 4, catalyst loading = 8%, reaction temperature = 160 °C, and reaction time = 80 min
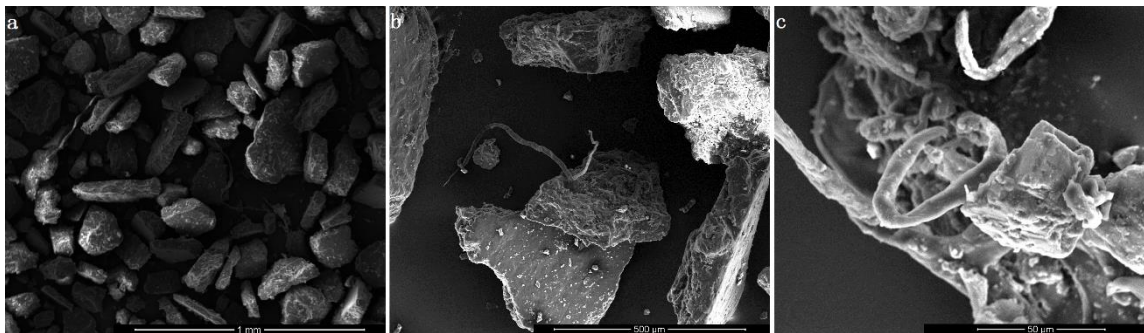
Fig. 5. SEM micrographs of the liquefaction products; liquefaction conditions: phenol/peanut shells ratio = 4, catalyst loading = 8%, reaction temperature = 160 °C, and reaction time = 80 min

CONCLUSIONS

In this study, peanut shells were effectively liquefied in phenol using sulfuric acid as a catalyst.

1. The results showed that the reaction conditions had different effects on the residue ratio, combined phenol, and formaldehyde reactivity.

2. During the liquefaction process, the lignin and hemicellulose were converted to methanol-soluble compounds, while less cellulose fiber was left in the residues.

3. The liquefied products contained a large amount of polyphenol compounds and a small quantity of furan compounds and furfural. This liquefaction process provides a potential approach to generate high-quality chemical feedstocks, which can be used directly to prepare bio-based phenolic resins.

ACKNOWLEDGMENTS

REFERENCES CITED

Ahmad, M., Lee, S. S., Dou, X., Mohan, D., Sung, J.-K., Yang, J. E., and Ok, Y. S. (2012). "Effects of pyrolysis temperature on soybean stover- and peanut shell-derived biochar properties and TCE adsorption in water," *Bioresource Technol.* 118, 536-544. DOI: 10.1016/j.biortech.2012.05.042

Ahmadzadeh, A., Zakaria, S., and Rashid, R. (2009). "Liquefaction of oil palm empty fruit bunch (EFB) into phenol and characterization of phenolated EFB resin," *Ind. Crop. Prod.* 30(1), 54-58. DOI: 10.1016/j.indcrop.2009.01.005

Alma, M., Yoshioka, M., Yao, Y., and Shiraishi, N. (1996a). "Phenolation of wood using oxalic acid as a catalyst: Effects of temperature and hydrochloric acid addition," *J. Appl. Polym. Sci.* 61(4), 675-683. DOI: 10.1002/(SICI)1097-

4628(19960725)61:4<675::AID-APP11>3.0.CO;2-X

Alma, M. H., Yoshioka, M., Yao, Y., and Shiraishi, N. (1996b). "The preparation and flow properties of HC1 catalyzed phenolated wood and its blends with commercial novolak resin," *Holzforschung* 50(1), 85-90. DOI: 10.1515/hfsg.1996.50.1.85

Alma, M. H., and Acemioglu, B. (2004). "A kinetic study of sulfuric acid-catalyzed liquefaction of wood into phenol," *Chem. Eng. Commun.* 191(7), 968-980. DOI: 10.1080/00986440490276173

Alma, M. H., and Basturk, M. A. (2006). "Liquefaction of grapevine cane (*Vitis vinisera* L.) waste and its application to phenol-formaldehyde type adhesive," *Ind. Crop. Prod.* 24(2), 171-176. DOI: 10.1016/j.indcrop.2006.03.010

Alma, M. H., and Kelley, S. S. (2002). "The application of pyrolysis-molecular beam mass spectrometry for characterization of bark phenolysis products," *Biomass Bioenerg.* 22(5), 411-419. DOI: 10.1016/S0961-9534(02)00018-1

Alma, M. H., Yoshioka, M., Yao, Y., and Shiraishi, N. (1998). "Preparation of sulfuric acid-catalyzed phenolated wood resin," *Wood Sci. Technol.* 32(4), 297-308. DOI: 10.1007/bf00702897

Biswas, B., Pandey, N., Bisht, Y., Singh, R., Kumar, J., and Bhaskar, T. (2017). "Pyrolysis of agricultural biomass residues: Comparative study of corn cob, wheat straw, rice straw and rice husk," *Bioresource Technol.* 237, 57-63. DOI: 10.1016/j.biortech.2017.02.046

Chu, G., Zhao, J., Chen, F., Dong, X., Zhou, D., Liang, N., Wu, M., Pan, B., and Steinberg, C. E. W. (2017). "Physi-chemical and sorption properties of biochars prepared from peanut shell using thermal pyrolysis and microwave irradiation," *Environ. Pollut.* 227, 372-379. DOI: 10.1016/j.envpol.2017.04.067

Effendi, A., Gerhauser, H., and Bridgwater, A. V. (2008). "Production of renewable phenolic resins by thermochemical conversion of biomass: A review," *Renew. Sust. Energ. Rev.* 12(8), 2092-2116. DOI: 10.1016/j.rser.2007.04.008

Feng, S., Yuan, Z., Leitch, M., Shui, H., and Xu, C. C. (2016). "Effects of bark extraction before liquefaction and liquid oil fractionation after liquefaction on bark-based phenol formaldehyde resoles." *Ind. Crop. Prod.* 84, 330-336. DOI: 10.1016/j.indcrop.2016.02.022

Feng, S., Yuan, Z., Leitch, M., and Xu, C. C. (2015). "Adhesives formulated from bark bio-crude and phenol formaldehyde resole," *Ind. Crop. Prod.* 76, 258-268. DOI: 10.1016/j.indcrop.2015.06.056

Feng, S., Cheng, S., Yuan, Z., Leitch, M., and Xu, C. C. (2013). "Valorization of bark for chemicals and materials: A review," *Renew. Sust. Energ. Rev.* 26, 560-578. DOI: 10.1016/j.rser.2013.06.024

Gao, F., Ye, H., Yu, Y., Zhang, T., and Deng, X. (2011). "Lack of toxicological effect through mutagenicity test of polyphenol extracts from peanut shells," *Food Chem.* 129(3), 920-924. DOI: 10.1016/j.foodchem.2011.05.046

GB/T 2677 .10 (1995). "Fibrous raw material – Determination of holocellulose." Standardization Administration of China, Beijing, China.

GB/T 2677 .8 (1994). "Fibrous raw material – Determination of acid – insoluble lignin, " Standardization Administration of China, Beijing, China.

GB/T 2677 .6 (1994). "Fibrous raw material – Determination of solvent extractives," Standardization Administration of China, Beijing, China.

GB/T 2677 .3 (1993). "Fibrous raw material – Determination of ash," Standardization Administration of China, Beijing, China.

GB/T 14074 (2006). "Testing methods for wood adhesives and their resins," Standardization Administration of China, Beijing, China.

Georgin, J., Dotto, G. L., Mazutti, M. A., and Foletto, E. L. (2016). "Preparation of activated carbon from peanut shell by conventional pyrolysis and microwave irradiation-pyrolysis to remove organic dyes from aqueous solutions," *Journal of Environment Chemical Engineering* 4(1), 266-275. DOI: 10.1016/j.jece.2015.11.018

Gurevich Messina, L. I., Bonelli, P. R., and Cukierman, A. L. (2015). "Copyrolysis of peanut shells and cassava starch mixtures: Effect of the components proportion," *J. Anal. Appl. Pyrol.* 113, 508-517. DOI: 10.1016/j.jaap.2015.03.017

Gurevich Messina, L. I., Bonelli, P. R., and Cukierman, A. L. (2017). "*In-situ* catalytic pyrolysis of peanut shells using modified natural zeolite," *Fuel Process. Technol.* 159, 160-167. DOI: 10.1016/j.fuproc.2017.01.032

Hassan, E. B., Kim, M., and Wan, H. (2009). "Phenol–formaldehyde-type resins made from phenol-liquefied wood for the bonding of particleboard," *J. Appl. Polym. Sci.* 112(3), 1436-1443. DOI: 10.1002/app.29521

Karagöz, S., Bhaskar, T., Muto, A., and Sakata, Y. (2004). "Effect of Rb and Cs carbonates for production of phenols from liquefaction of wood biomass," *Fuel* 83(17-18), 2293-2299. DOI: 10.1016/j.fuel.2004.06.023

Lee, W.-J., Kang, C.-L., Chang, K.-C., and Chen, Y.-C. (2012). "Synthesis and properties of resol-type phenol-formaldehyde resins prepared from H_2SO_4-and HCl-catalyzed phenol-liquefied *Cryptomeria japonica* wood," *Holzforschung* 66(1), 67-72. DOI: 10.1515/HF.2011.121

Li, G.-Y., Hse, C.-Y., and Qin, T.-F. (2012). "Preparation and characterization of novolak phenol formaldehyde resin from liquefied brown-rotted wood," *J. Appl. Polym. Sci.* 125(4), 3142-3147. DOI: 10.1002/app.36476

Lin, L., Yao, Y., Yoshioka, M., and Shiraishi, N. (1997). "Molecular weights and molecular weight distributions of liquefied wood obtained by acid-catalyzed phenolysis," *J. Appl. Polym. Sci.* 64(2), 351-357. DOI: 10.1002/(sici)1097-4628(19970411)64:2<351::Aid-app16>3.0.Co;2-3

Lin, L., Yoshioka, M., Yao, Y., and Shiraishi, N. (1994). "Liquefaction of wood in the presence of phenol using phosphoric acid as a catalyst and the flow properties of the liquefied wood," *J. Appl. Polym. Sci.* 52(11), 1629-1636. DOI: 10.1002/app.1994.070521111

Long, J., Lou, W., Wang, L., Yin, B., and Li, X. (2015). "[$C_4H_8SO_3Hmim$]HSO_4 as an efficient catalyst for direct liquefaction of bagasse lignin: Decomposition properties of the inner structural units," *Chem. Eng. Sci.* 122, 24-33. DOI: 10.1016/j.ces.2014.09.026

Mamaeva, A., Tahmasebi, A., and Yu, J. (2017). "The effects of mineral salt catalysts on selectivity of phenolic compounds in bio-oil during microwave pyrolysis of peanut shell," *Korean J. Chem. Eng.* 34(3), 672-680. DOI: 10.1007/s11814-016-0291-3

Pan, H., Shupe, T. F., and Hse, C.-Y. (2007). "Characterization of liquefied wood residues from different liquefaction conditions," *J. Appl. Polym. Sci.* 105(6), 3739-3746. DOI: 10.1002/app.26435

Pan, H., Shupe, T. F., and Hse, C.-Y. (2009). "Characterization of novolac type liquefied wood/phenol/formaldehyde (LWPF) resin," *Eur. J. Wood Wood Prod.* 67(4), 427-437. DOI: 10.1007/s00107-009-0337-x

Ping, L., Brosse, N., Sannigrahi, P., and Ragauskas, A. (2011). "Evaluation of grape stalks as a bioresource," *Ind. Crop. Prod.* 33(1), 200-204. DOI:

10.1016/j.indcrop.2010.10.009

Pizzi, A. (2006). "Recent developments in eco-efficient bio-based adhesives for wood bonding: Opportunities and issues," *J. Adhes. Sci. Technol.* 20(8), 829-846. DOI: 10.1163/1568561067777638635

Ragauskas, A. J., Williams, C. K., Davison, B. H., Britovsek, G., Cairney, J., Eckert, C. A., Frederick Jr., W. J., Hallett, J. P., Leak, D. J., Liotta, C. L., *et al*. (2006). "The path forward for biofuels and biomaterials," *Science* 311(5760), 484-489. DOI: 10.1126/science.1114736

Wu, M.-b., Li, R.-c., He, X.-j., Zhang, H.-b., Sui, W.-b., and Tan, M.-h. (2015). "Microwave-assisted preparation of peanut shell-based activated carbons and their use in electrochemical capacitors," *New Carbon Mater.* 30(1), 86-91. DOI: 10.1016/S1872-5805(15)60178-0

Xu, W., Zhao, Q., Wang, R., Jiang, Z., Zhang, Z., Gao, X., and Ye, Z. (2017). "Optimization of organic pollutants removal from soil eluent by activated carbon derived from peanut shells using response surface methodology," *Vacuum* 141, 307-315. DOI: 10.1016/j.vacuum.2017.04.031

Yan, N., Zhang, B., Zhao, Y., Farnood, R. R., and Shi, J. (2017). "Application of biobased phenol formaldehyde novolac resin derived from beetle infested lodgepole pine barks for thermal molding of wood composites," *Ind. Eng. Chem. Res.* 56(22), 6369-6377. DOI: 10.1021/acs.iecr.7b00353

Yang, H., Yan, R., Chen, H., Lee, D. H., and Zheng, C. (2007). "Characteristics of hemicellulose, cellulose and lignin pyrolysis," *Fuel* 86(12-13), 1781-1788. DOI: 10.1016/j.fuel.2006.12.013

Yao, Q., Li, S.-Q., Xu, H.-W., Zhuo, J.-K., and Song, Q. (2010). "Reprint of: Studies on formation and control of combustion particulate matter in China: A review," *Energy* 35(11), 4480-4493. DOI: 10.1016/j.energy.2010.08.009

Zhang, A., Li, J., Zhang, S., Mu, Y., Zhang, W., and Li, J. (2017a). "Characterization and acid-catalysed depolymerization of condensed tannins derived from larch bark," *RSC Adv.* 7(56), 35135-35146. DOI: 10.1039/C7RA03410E

Zhang, C., Zhang, R., Li, X., Li, Y., Shi, W., Ren, X., and Xu, X. (2011). "Bench-scale fluidized-bed fast pyrolysis of peanut shell for bio-oil production," *Environ. Prog. Sustain.* 30(1), 11-18. DOI: 10.1002/ep.10530

Zhang, G., Hu, M., He, L., Fu, P., Wang, L., and Zhou, J. (2013). "Optimization of microwave-assisted enzymatic extraction of polyphenols from waste peanut shells and evaluation of its antioxidant and antibacterial activities *in vitro*," *Food Bioprod. Process.* 91(2), 158-168. DOI: 10.1016/j.fbp.2012.09.003

Zhang, G., Zhang, Q., Wu, Y., Zhang, H., Cao, J., and Han, D. (2017b). "Effect of auxiliary blowing agents on properties of rigid polyurethane foams based on liquefied products from peanut shell," *J. Appl. Polym. Sci.* 134(48). DOI: 10.1002/app.45582

Zhang, J., Wang, R., Cao, X., Li, Y., and Lan, Y. (2014). "Preparation and characterization of activated carbons from peanut shell and rice bran and a comparative study for Cr(VI) removal from aqueous solution," *Water Air Soil Poll.* 225(7), 2032-2041. DOI: 10.1007/s11270-014-2032-8

Zhang, Q., Zhang, G., Han, D., and Wu, Y. (2016). "Renewable chemical feedstocks from peanut shell liquefaction: Preparation and characterization of liquefied products and residue," *J. Appl. Polym. Sci.* 133(44). DOI: 10.1002/app.44162

Zhang, Y., Ikeda, A., Hori, N., Takemura, A., Ono, H., and Yamada, T. (2006). "Characterization of liquefied product from cellulose with phenol in the presence of

sulfuric acid," *Bioresource Technol.* 97(2), 313-321. DOI: 10.1016/j.biortech.2005.02.019

Zhao, Y., Yan, N., and Feng, M. W. (2013). "Effects of reaction conditions on phenol liquefaction of beetle-infested lodgepole pine barks," *Curr. Org. Chem.* 17(15), 1604-1616. DOI: 10.2174/13852728113179990070

Zhong, Z.-Y., Yang, Q., Li, X.-M., Luo, K., Liu, Y., and Zeng, G.-M. (2012). "Preparation of peanut hull-based activated carbon by microwave-induced phosphoric acid activation and its application in Remazol Brilliant Blue R adsorption," *Ind. Crop. Prod.* 37(1), 178-185. DOI: 10.1016/j.indcrop.2011.12.015